



## RESEARCH ARTICLE OPEN ACCESS

# Evaluation of the Mechanical and Physical Behaviors of Flax Fiber-Reinforced Polybutylene Succinate Biodegradable Composites in Packaging Applications

Sema Özalp<sup>1</sup>  | Sedef Sismanoglu<sup>2</sup>  | Ümit Tayfun<sup>3</sup>  | Carmen-Mihaela Popescu<sup>4,5,6</sup>  | Fazilat B. Kairliyeve<sup>7</sup>  | Yasin Kanbur<sup>2</sup> 

<sup>1</sup>Metallurgical and Materials Engineering, Karabuk University, Karabük, Türkiye | <sup>2</sup>Department of Chemistry, Karabuk University, Karabük, Türkiye | <sup>3</sup>Basic Sciences, Bartın University, Bartın, Türkiye | <sup>4</sup>Petru Poni Institute of Macromolecular Chemistry of the Romanian Academy, Iasi, Romania | <sup>5</sup>School of Computing, Engineering and Built Environment, Edinburgh Napier University, Edinburgh, UK | <sup>6</sup>Rural Development Research Platform, Iasi, Romania | <sup>7</sup>Chemical Technology of Organic Substances, Atyrau Oil and Gas University, Atyrau, Kazakhstan

**Correspondence:** Yasin Kanbur ([yasinkanbur@karabuk.edu.tr](mailto:yasinkanbur@karabuk.edu.tr))

**Received:** 24 April 2025 | **Revised:** 25 June 2025 | **Accepted:** 30 June 2025

**Funding:** This study was supported by Karabuk University Scientific Research Projects (BAP) Coordination Office with the project numbered KBÜBAP-21-YL-002.

**Keywords:** biocomposites | biodegradable packaging material | composite films | flax fiber | polybutylene succinate

## ABSTRACT

Applying surface modification routes to natural fibers is a practical option for solving the incompatibility problem in polymeric composites. This study aimed to improve the properties of biodegradable and environmentally friendly polybutylene succinate (PBS) composites involving flax fiber (FF) with unmodified, alkalization, and silanization surface modification applied at 20 wt%. The surface modifications were successfully characterized by FTIR and SEM. The composites were prepared using a twin-screw extruder followed by injection molding. The mechanical, thermal, thermo-mechanical, wear, water absorption, biodegradation, and morphological properties were evaluated. The incorporation of FF improved the mechanical and thermal performance of PBS, while the surface modifications further increased the fiber-matrix adhesion. In particular, the silanized FF provided water resistance due to the hydrophobic nature of siloxane and exhibited the lowest biodegradation rate under fungal exposure. In the case of silanized FF, a 5.4% improvement in tensile strength and nearly 3% of water absorption capacity were reached. Based on these outcomes, the silanized FF-filled PBS composite was suitable for packaging applications where biodegradable, water-resistant, and mechanically strong materials are required.

## 1 | Introduction

In recent years, environmentally friendly polymer materials produced from renewable sources have attracted attention. The main reasons for this interest are their long decomposition periods and the serious environmental problems caused by single-use plastic waste. These issues pose significant challenges and storage problems for governments and manufacturers. Such disadvantages have spurred researchers and manufacturers into action. The incorporation of biodegradable polymers, which can

undergo biodegradation, with other materials (synthetic or natural) to obtain sustainable, natural, and environmentally friendly materials has proven to be a cost-effective and efficient solution [1, 2].

The reasons for using such natural fillers include their economic viability, lightweight nature, minimal damage to processing equipment, abundance as a resource, biodegradability, excellent surface quality of molded parts, and favorable mechanical properties. Various types of natural fibers are currently being

This is an open access article under the terms of the [Creative Commons Attribution](https://creativecommons.org/licenses/by/4.0/) License, which permits use, distribution and reproduction in any medium, provided the original work is properly cited.

© 2025 The Author(s). *SPE Polymers* published by Wiley Periodicals LLC on behalf of Society of Plastics Engineers.

## Summary

- Polybutylene-succinate was compounded by neat and surface-treated flax fiber.
- PBS-based biodegradable composites were produced via the melt-blending process.
- Silane modification of FF improved mechanical and thermal characteristics.
- Composite involving silane-treated FF yielded a decline in biodegradation rate.

researched for use in composites. Natural fibers have been increasingly used in the past decade due to their ability to biodegrade, recyclability, and especially their nonharmful nature to the human body [3, 4].

Flax fiber, one of the main lignocellulosic fibers, contains cellulose, hemicellulose, pectin, lignin, oil and wax, protein, and small amounts of inorganic substances. Pectin and lignin are two crucial components that affect the whole microstructure. The use of natural fibers in studies to strengthen composite materials has increased in recent years. Polymer composites reinforced with environmentally friendly, biodegradable flax fiber are useful in many industrial areas. Flax fiber-reinforced eco-composites have gained a place in the automotive, textile, and packaging sectors [5–8].

Numerous studies have shown that the mechanical performance of flax fiber-reinforced composites depends on various factors, including fiber surface treatment, type of matrix, and composite processing methods. Surface treatments like alkali and silane treatment enhance mechanical properties by improving the interfacial adhesion between flax fibers and polymer matrices [9–13]. Beside this, the polymer matrix plays a crucial role in determining the overall performance of the composite. Especially, biodegradable polymers like polylactic acid (PLA) and polybutylene succinate (PBS), as well as polyhydroxybutyrate (PHB), demonstrate promising results regarding mechanical strength and biodegradability [9, 14, 15]. The biodegradation of flax fiber composites is another critical area studied in the literature. Including flax fibers in the polymer matrices significantly increases the composites' biodegradability and makes them suitable for environmentally sensitive applications [16, 17]. Flax fibers provide a higher degradation rate than synthetic alternatives, and the decomposition rate of the composites varies depending on the amount of fiber, matrix type, and environmental conditions [16]. Due to this, flax fiber-reinforced composites can be used in various industries, including the construction, automotive, and packaging fields [18, 19].

The hydrophobic nature of the flax fiber limited the performance of the PBS-based composites due to the poor compatibility between flax fiber and PBS [20, 21]. Surface modification is the most common method to improve flax fiber's interaction with PBS and raise the mechanical and barrier qualities of the resultant composites. The main purpose of surface modifications applied to flax fiber is to increase the interfacial adhesion of the fiber-PBS matrix and the roughness of the fiber surface. When studies using flax fiber as a filler are examined,

it is seen that a wide variety of surface modifications are used [22–26]. It has been observed that alkalization and silanization surface modifications improve the mechanical properties of the composites [22–26]. Alkali treatment, plasma modification, or gamma irradiation of flax fibers increases the surface roughness and chemical reactivity, improving adhesion inside the polymer matrix [27–30]. Another good choice to serve better surface compatibility is silanization of flax fiber surface [12]. Higher performance of food packaging products is due to composites with both increased mechanical strength and reduced water vapor permeability, which can only be achieved with better interfacial bonding [20, 31]. For this reason, alkalization and silanization surface modifications were applied to flax fiber in our study.

Using renewable agricultural resources like flax fibers in PBS matrices helps reinforce the composite mechanically and adheres to sustainability principles [20, 32]. Additionally, the biodegradability of both ingredients provides a short breakdown of composites organically in nature and reduces the environmental impact of conventional plastics derived from petroleum [21, 33, 34].

Aliphatic polyesters are polymers that are considered biodegradable and environmentally friendly. Polybutylene succinate (PBS) is one of the most chemically promising aliphatic polyesters. In recent years, there has been an increase in the use of PBS and other bio-based polymers. PBS is a commercially available, low-cost polymer with many interesting properties, including biodegradability, high elasticity, chemical and thermal resistance, and melt processability [35–38].

When the studies conducted in the literature to date are examined, natural fibers such as alpha fiber, cotton fiber, and rice straw fiber were added to the PBS matrix as filler by alkalizing and silanization surface modifications, and a strong surface bonding was observed [20]. As a result of adding pure kenaf fiber to PBS, it was observed that there was a phase separation between PBS and kenaf fiber [20]. In another study, it was observed that there was an increase in Young's modulus when flax fiber was added to the PBS matrix at a rate of 25.5% by weight [39]. It was observed that the Young's modulus and tensile strength of the composites increased with the addition of 20% of pure flax fiber to the polymer matrix consisting of 80% PLA and 20% PBS by weight [40]. It was observed that the mechanical properties of the composites increased with the addition of 20% flax fiber with alkalizing surface modification to the polymer matrix consisting of 80% PLA and 20% PBS by lamination method [41]. It is known that surface modifications solve surface adhesion problems and accordingly improve the mechanical properties of the composites. In previous studies, flax fiber without modification was added to PBS/PLA polymer blends or pure PBS as filler [20, 39, 40]. Flax fiber with surface modification by alkalization was added to PBS/PLA polymer blend by lamination method [41].

The objective of the study was to examine the impact of surface-modified flax fiber on the characteristics of PBS composites meant for packaging applications. Two different surface modifications were applied to flax fiber: alkylation and silanization. The prepared composites were examined with scanning electron microscopy (SEM), tensile test, biodegradation test, and thermal

gravimetric analysis to evaluate the effects of surface treatment on mechanical strength, thermal stability, water absorption, biodegradation rates, and the general morphology of the composite materials. Integrating FF into the PBS matrix effectively led to an increase in biomass content of the resulting composites, which is suited for fabricating flexible bio-based film products for packaging applications.

## 2 | Experimental

### 2.1 | Materials

Polybutylenesuccinate (polybutylenesuccinate) ( $d_{\text{PBS}} = 1.26 \text{ g/cm}^3$ ; MFR (190°C, 2.16 kg) = 22 g/10 min; tensile strength = 30–40 MPa) was purchased from PTT Global Chemical Public Company Limited (GC) with the trade name of FZ79AC. NM 4.8/1—NM 6/1 semi-wet spun natural FF yarns were supplied from Filofibra Pazarlama A.Ş. Sodium hydroxide (NaOH) purchased from Sigma Aldrich, was used for alkalization. Ethyl alcohol, used in silanization surface modification, was obtained from Merck. [3-(2,3-epoxypropoxy)-propyl]-trimethoxysilane was purchased from Alfa Aesar.

### 2.2 | Surface Treatment of FF

The flax fibers were cut into 3–4 mm lengths with the help of a pair of scissors. During alkalization surface modification, flax fibers were stirred in a 2% (w/v) NaOH/water solution for 2 h at room temperature. After stirring, the mixture was washed several times with distilled water. A few drops of acetic acid were used to remove the residual NaOH in the medium. After this process, the sample was dried in an oven at 100°C for 240 min and labeled Na-FF. In silanation surface modification, flax fiber was stirred in a 4% (v/v) (3-(2,3-epoxypropoxy)-propyl)-trimethoxysilane/ethanol solution for 120 min at room temperature. The sample was washed several times with ethanol, dried in an oven at 80°C for 240 min, and coded Si-FF. The sample without surface treatment was labeled as FF.

### 2.3 | Production of Composites

The most commonly used method to ensure a homogeneous mixture in the production of thermoplastic polymer composites is mixing in a twin screw extruder [42]. The twin-screw extrusion method is also a high-shear method used to ensure optimum fiber distribution [22]. PBS without additives and PBS/flax fiber samples were mixed in a twin-screw micro-extruder (MC15 HT, Xplore Instruments) at 200°C and 100 rpm for 5 min. The added amount of FF was kept constant at 20 wt% in the prepared composites. The maximum weight capacity of the extruder used in the study is 15 g. For mixing each composite sample, 3 g was weighed for each set and 12 g of PBS was added. After mixing three sets separately for each composite material, the inside of the twin screw extruder was cleaned with pure PBS. Injection molding is the most suitable production shaping method for thermoplastic materials [43]. For tensile, water absorption, and abrasion tests, the specimens were shaped using an injection molding machine (Micro-injector, Daga) with a

barrel temperature of 210°C, a mold temperature of 30°C and a pressure of 8 bar.

## 2.4 | Characterization Techniques

FTIR analysis of FF fibers with and without surface modification was performed using an IR-spectrometer device (Bruker Alpha FT-IR Spectrometer and Microscope) between 4500 and 500  $\text{cm}^{-1}$  wave numbers. FESEM images for surface characterization of FF fibers with and without surface modification and morphological properties of fracture surfaces of composites were obtained by coating fibers and fracture surfaces with gold, using a Carl Zeiss Ultra Plus Gemini brand field effect scanning electron microscope (FESEM) device at  $\times 1000$  and  $\times 5000$  magnifications. Tensile tests of composite materials before and after the water absorption test were performed using a universal tensile testing machine (Lloyd LR 30 K) with a 5 kN load cell at a tensile speed of 5  $\text{cm min}^{-1}$  in accordance with the ASTM D-638 standard. The standard deviation calculation in tensile test values was made by taking the average of the four tested samples. TGA analysis of PBS and composite structures was performed on Hitachi STA 7300 Thermogravimetric Analyzer between 25°C and 600°C at a heating rate of 10°C/min. In order to determine the water absorption properties of the composites, they were conditioned in accordance with the ASTM D570 procedure. After the standard tensile test samples were immersed in a room temperature water bath for a certain time, they were removed from the water, wiped to remove surface water, and weighed again, then placed back in water. The water absorption capacities of the samples ( $W_0$ ) whose dry weight was previously weighed were calculated according to the formula shown in Equation (1).

$$\text{Water absorption (\%)} = \frac{W_f - W_0}{W_0} \times 100 \quad (1)$$

$W_f$  shown in the formula shows the weight of the samples after immersion in water.

The samples were subjected to wear tests according to ASTM G133 standard. In this application, UTS Tribometer T10 wear tester was used. The test application was carried out reciprocating a 5 N weight, 10 mm stroke, and 20 m total sliding distance. The thermo-mechanical properties of the composites were determined by a dynamic mechanical thermal analyzer (DMA 8000, Perkin Elmer) between  $-100^\circ\text{C}$  and  $100^\circ\text{C}$  in double cantilever tilt mode, at a fixed frequency of 1 Hz and a heating rate of 10°C/min.

## 3 | Results and Discussion

### 3.1 | Surface Properties of FF

The spectra of unmodified and modified flax fibers are presented in Figure 1. The spectrum of unmodified fibers presents a typical spectrum of annual fiber crops containing cellulose, hemicelluloses, and lignin with two main regions (3700 and 2700  $\text{cm}^{-1}$  region and 1800–500  $\text{cm}^{-1}$  region). The first region presents a large band with two maxima at 3331 and 3289  $\text{cm}^{-1}$ ,

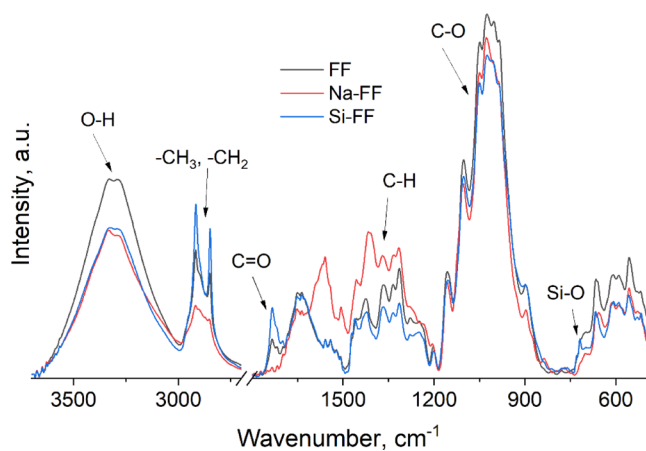
assigned to different intra- and intermolecular hydrogen bonds from cellulose structure, and two sharp bands at 2917 and 2840  $\text{cm}^{-1}$  assigned to symmetric and antisymmetric stretching vibrations of methyl and methylene groups [44, 45].

In the second region, main bands are observed at: 1733  $\text{cm}^{-1}$  assigned to C=O from acetyl and carboxyl groups mainly from hemicelluloses, 1641  $\text{cm}^{-1}$  assigned to absorbed water molecules, as well as to C=O stretching vibration from carboxyl groups, 1550  $\text{cm}^{-1}$  assigned to stretching vibration of conjugated C—O groups, 1459, 1425, and 1366  $\text{cm}^{-1}$  assigned to C—H deformation vibration in lignin and carbohydrates, 1335  $\text{cm}^{-1}$  C—H assigned to stretching vibration in cellulose and C<sub>1</sub>—O stretching vibration in syringyl derivatives, 1314  $\text{cm}^{-1}$  assigned to CH<sub>2</sub> rocking vibration in cellulose, 1278  $\text{cm}^{-1}$  assigned to C—H bending mode in cellulose and C—O stretch in lignin, 1249  $\text{cm}^{-1}$  assigned to C—O stretching vibration in lignin and hemicelluloses and C—O—C stretching mode of the pyranose ring, 1204  $\text{cm}^{-1}$  C=O stretching vibration in lignin and xylan, 1157  $\text{cm}^{-1}$  assigned to C—O—C stretching vibration in carbohydrates, 1102, 1051, 1025, 1003, and 983  $\text{cm}^{-1}$  assigned to C—O stretching vibration in carbohydrates, and at 897  $\text{cm}^{-1}$  assigned to C—H deformation in cellulose [44, 45].

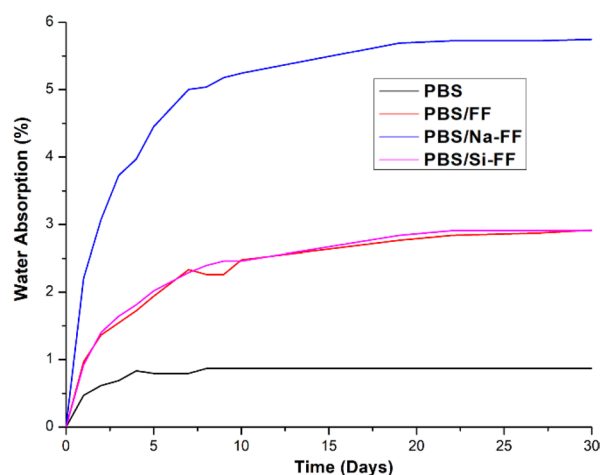
The spectrum of the Na-FF presents few differences compared to untreated fibers, such as: the band from 1731  $\text{cm}^{-1}$  is reduced in intensity, the band from 1560  $\text{cm}^{-1}$  shows stronger

intensity, while 1507  $\text{cm}^{-1}$  is better defined. Further, the band from 1412  $\text{cm}^{-1}$  is shifted from 1452  $\text{cm}^{-1}$ ; the bands from 1317, 1003, and 987  $\text{cm}^{-1}$  have reduced intensity, indicating the modification of the fibers. The main difference in the Si-FF spectrum shows the band from 725  $\text{cm}^{-1}$  assigned to Si—O bond stretching vibrations [46, 47]. Reduced intensities indicate a reduced amount of groups that vibrate at a certain wavenumber, while increased intensities indicate an increased amount of groups that vibrate at a certain wavenumber. Moreover, it is known that the main water sorption sites are OH groups but also the C=O groups. The modifications indicate a reduced amount of C=O and C—O groups in carbohydrates and an increased amount of conjugated C—O groups. These indicate a reduction in the water sorption sites. Moreover, the Si-FF spectrum clearly indicates the formation of Si—O bonds at the surface of the fibers, also indicating the hydrophobisation of the fibers.

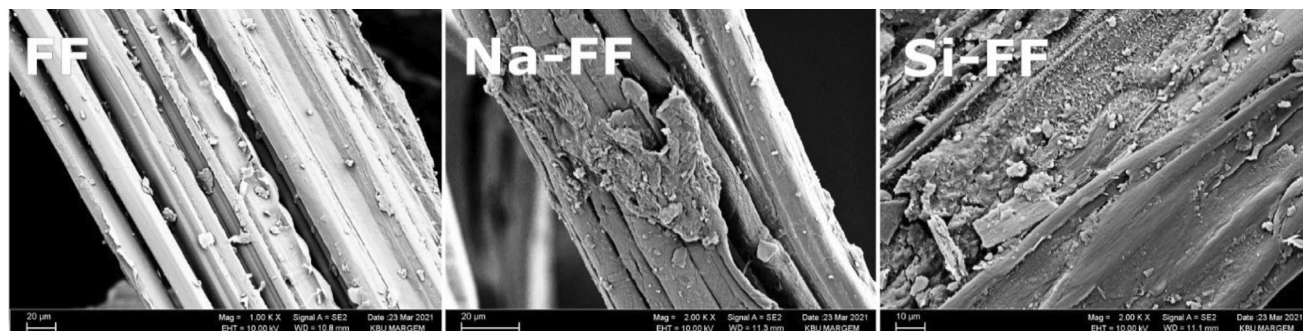
When the FESEM images of the FF with and without surface modification are examined in Figure 2, it is seen that the structure of the FF without surface modification is flatter and smoother, while more amorphous structures with more indentations and protrusions are formed on the flat fiber surface with alkalization. As a result of the silanization surface modification, it is seen that non-cellulosic substances such as lignin, hemicellulose, and pectin are removed from the structure, the FF is coated with silanes, and the structure becomes rougher.



**FIGURE 1** | Infrared spectra of the untreated and treated flax fibers in the 3700–500  $\text{cm}^{-1}$  region.



**FIGURE 3** | Water absorption curves of PBS and PBS/FF composites.

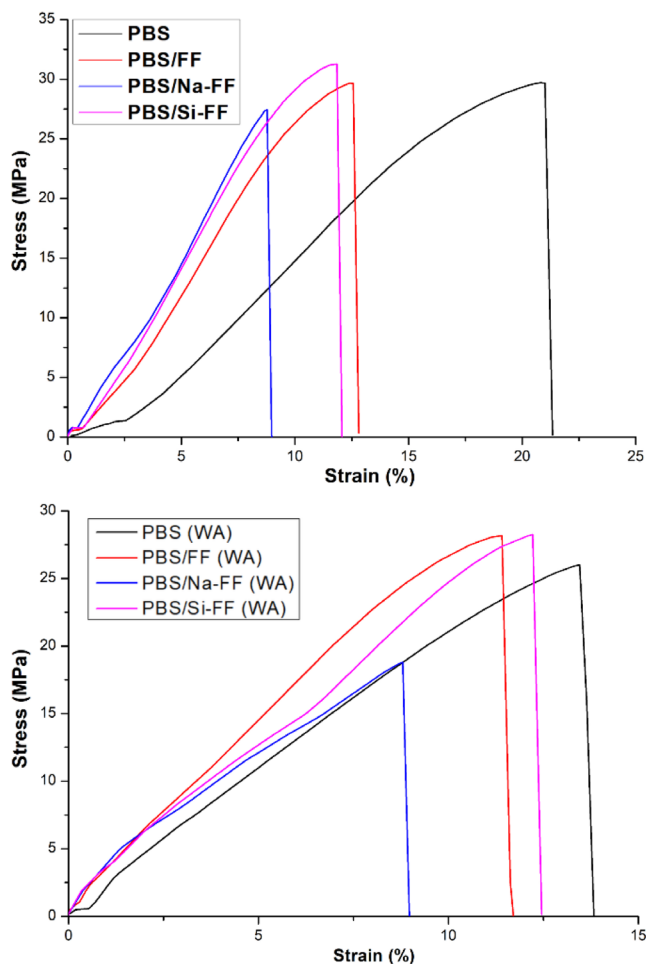


**FIGURE 2** | FESEM images of FF samples without and with surface modification.



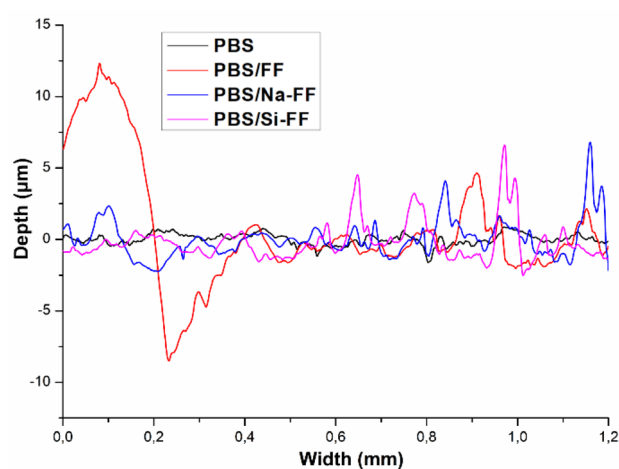
**TABLE 1** | Tensile properties of PBS and PBS/FF composites before and after water absorption test.

Samples	Tensile strength (MPa)	Percent strain at break (%)	Young's modulus (MPa)
PBS	$29.8 \pm 1.7/26.0 \pm 1.4^a$	$20.9 \pm 1.2/13.6 \pm 1.4^a$	$201.9 \pm 0.8/370.4 \pm 1.2^a$
PBS/FF	$29.7 \pm 1.3/28.2 \pm 0.9^a$	$12.4 \pm 1.5/11.5 \pm 1.6^a$	$332.9 \pm 1.4/378.8 \pm 1.7^a$
PBS/Na-FF	$27.5 \pm 1.1/18.8 \pm 1.5^a$	$11.8 \pm 1.3/8.8 \pm 1.7^a$	$388.9 \pm 1.3/522.9 \pm 1.6^a$
PBS/Si-FF	$31.3 \pm 1.3/28.3 \pm 1.6^a$	$11.8 \pm 1.2/12.2 \pm 1.1^a$	$361.1 \pm 1.7/552.8 \pm 0.8^a$

<sup>a</sup>After the water absorption test.**FIGURE 4** | Tensile test graphs of PBS and composites.

### 3.2 | Water Resistance of Composites

The graph of water absorption capacities of PBS and composites is given in Figure 3. In the 32-day water absorption test, pure PBS's water absorption value reached a certain level within a 5 days and then stabilized at 0.7% throughout the test. The composites containing Na-FF showed the highest water absorption capacity with an average of 5.7% at the end of the test due to the formation of microvoids between the fiber surface and the polymer matrix. ES-FF and PBS-FF containing composites showed a water absorption capacity of 3%. Due to its hydrophobic character, silane-coated FF exhibited a noticeable decrease in the water absorption capacity of the composite [48–51]. PBS is formed by the polycondensation reaction of 1,4-butanediol and succinic acid [52]. It is thought that the —OH groups in the

**FIGURE 5** | Two-dimensional surface area plots of the worn surfaces of PBS/FF composites.

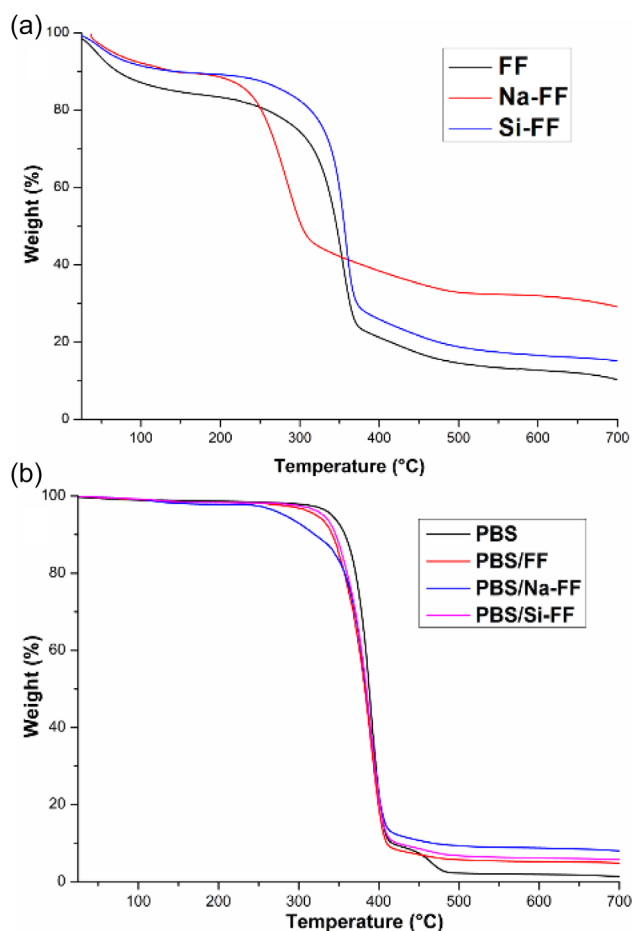
alcohol and succinic acid in the chemical structure of PBS are formed by the addition of silanization surface modified FF to form Si—OH bonds. Accordingly, it is observed that the water absorption of the composite decreases. Similarly, it is thought that the —OH groups in PBS combine with —H in the alkalization surface modification with NaOH and reduce the water absorption capacity as a result of removing water molecules from the environment.

### 3.3 | Tensile Behaviors of Composites

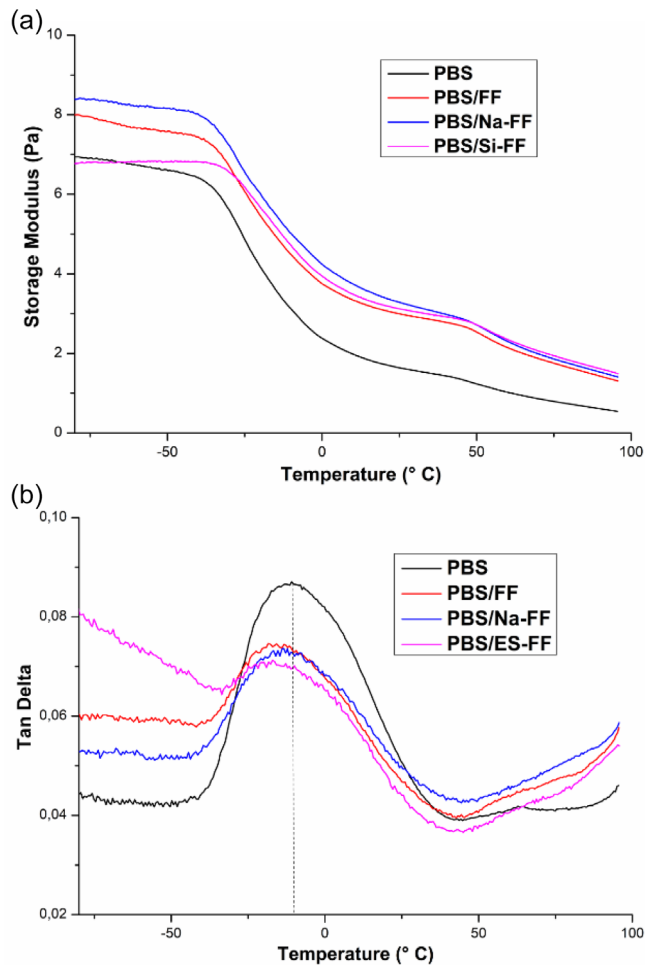
The tensile test results of PBS and composites before and after the water absorption test are listed in Table 1. The characteristic tensile strength curves of the composite specimens before (a) and after (b) the water absorption test are presented in Figure 4. With the addition of unmodified FF to the PBS matrix, there was no significant difference in tensile strength and an average decrease in percentage elongation close to 1.68 times compared to pure PBS. As another observation, an average increase of 1.65 times in Young's modulus was observed. When the composites with FF content with surface modification were compared with the composite filled with unmodified FF, it was deduced that the tensile strength of the composites with surface modification was higher. PBS/Si-FF composite showed the best improvement in tensile strength (5.39%) among all composites. The results can be attributed to the silanisation process, which enhances the interfacial interactions between FF and PBS [53, 54]. After the water absorption test, no significant change was found in the mechanical properties of pure PBS. At the same time, the examination of the

**TABLE 2** | Wear test parameters of PBS and PBS/FF composites.

Samples	Stroke (mm)	Surface area of wear (A) (cm <sup>2</sup> )	Specific wear rate ( $W_R$ ) (mm <sup>3</sup> /Nm)
PBS	10.0 ± 0.2	5.0 ± 0.3	0.01
PBS/FF	10.2 ± 0.2	50.3 ± 0.6	0.1
PBS/Na-FF	10.1 ± 0.2	20.7 ± 0.4	0.04
PBS/ES-FF	10.0 ± 0.2	8.6 ± 0.5	0.016

**FIGURE 6** | TGA curves of FF (a) and composites (b).

composites showed that significant changes occurred in their mechanical properties. An increase in the Young's modulus of PBS-based composites was observed after the water absorption test. Young's modulus is a measure of stiffness [55]. It was observed that the Young's modulus of composites containing unmodified and modified FF was higher than that of pure PBS before the water absorption test. When the tensile data before the water absorption test were examined, it was observed that the percent strain at break (%) values were lower than that of pure PBS with the increase in the Young's modulus. This suggests that the hardness values of the composites increased with the increase in the Young's modulus. The decrease in the percent elongation at break of the samples or their being almost similar with the increase in both pure PBS and various FF-containing composites after the water absorption test also shows that the results are consistent with each other.

**FIGURE 7** | Storage modulus: (a)  $\tan \delta$ , (b) curves of PBS and PBS/FF composites.

### 3.4 | Wear Measurements

Figure 5 shows the two-dimensional surface area diagram of the worn surfaces of PBS/FF composites. Table 2 shows the wear properties ratios of PBS and PBS/FF composite structures. The higher the specific wear value, the lower the wear resistance [56, 57].

The fibrous structure of FF increased the wear depth on the surface by facilitating particle breakage, which caused a decrease in wear resistance. With the addition of FF with or without a modification process to pure PBS, it was observed that the specific wear values increased and the wear resistance decreased due to this situation. The PBS/Na-FF composite showed that the

specific wear values decreased with the NaOH surface modification process compared to PBS/FF and, therefore, the wear resistance increased. As the composites were compared, the specific wear value of the composite modified with silanization showed the best improvement (60%).

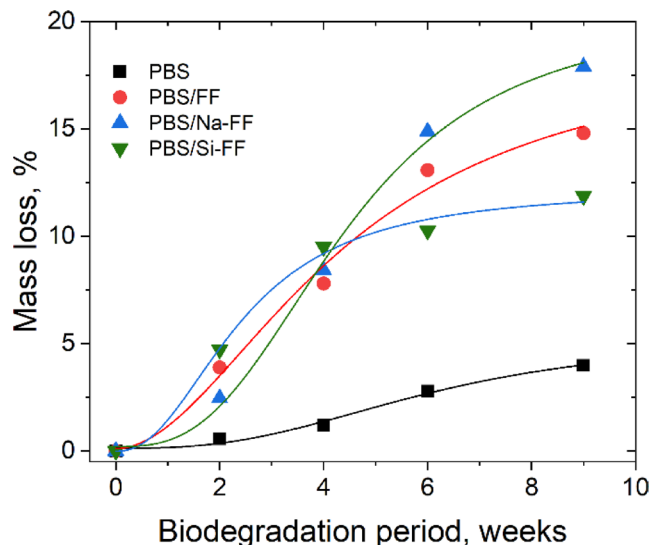


**FIGURE 8** | Mass loss recorded during the 9 weeks of the biodegradation period.

### 3.5 | Thermal Stability of Composites

Figure 6a displays that the untreated FF contains around 15% moisture, and alkali and silane modifications were found to reduce the moisture content in the fiber content below 10% since the decrease in the TGA curves between room temperature and 100°C indicates the moisture content of the samples. Alkali modification caused a significant reduction in the thermal degradation temperature, as it removed the cellulosic compounds in the FF structure [58–60]. However, the degradation rate of Na-FF was found to be slower compared to other samples. ES-FF and FF samples showed almost the same thermal degradation behavior.

According to the TGA curves of PBS and composites shown in Figure 6b, PBS exhibits a single-step thermal degradation curve around 350°C, starting with the separation of the succinate group in its structure [32, 61–63]. When the TGA curves of the composites containing FF are examined, it is noticeable that the PBS/Na-FF sample starts thermal degradation significantly earlier with respect to PBS and other composites. Silane-treated FF slightly increased the thermal strength of the composite. Compared to PBS without additives, the composites exhibited lower thermal strength at the beginning of the thermal degradation. The most prominent of these was determined as the composite sample containing alkali-modified FF. At the end temperature of thermal decomposition, almost 97.5% mass loss was observed in pure PBS. At

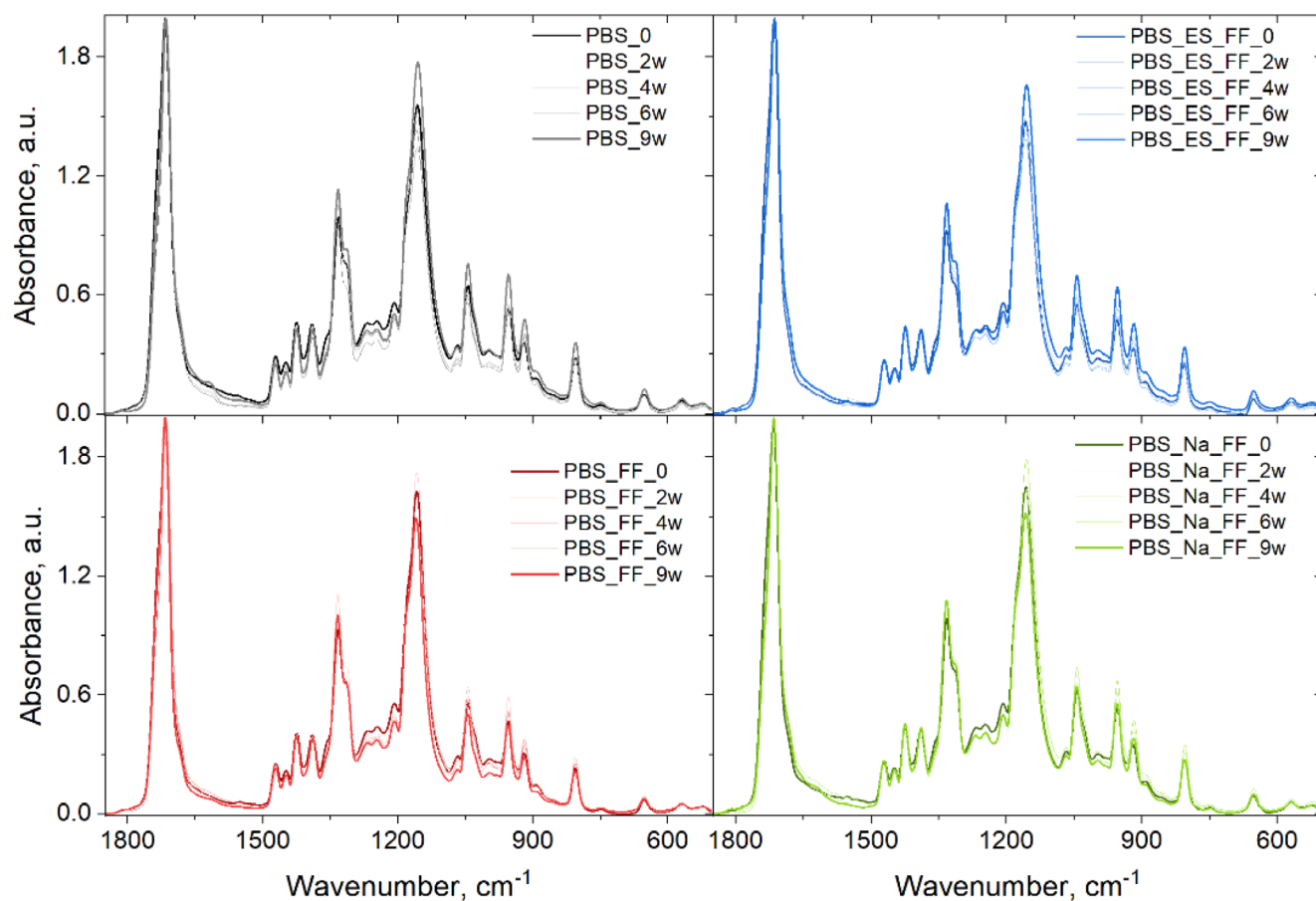


**FIGURE 9** | Infrared spectra in the 1830–500 cm<sup>-1</sup> of the polymer and its composites.



the end of the thermal decomposition step (approximately 490°C), mass percent amounts of unmodified FF, silane modified FF, and alkali modified FF were found to be 7.5%, 8.9%, and 10.2%, respectively. It was observed that unmodified and modified FF increased the thermal resistance of pure PBS. It is thought that alkalization surface modification causes rapid mass loss at the beginning of thermal degradation in both powder and composites because it increases the thermal degradation of cellulose in the structure of flax fiber. After the rapid degradation of cellulose in the structure of FF, the structure becomes more stable and mass losses decrease. For this reason, while the thermal resistance of composites containing Na-FF is lower at the beginning of thermal degradation, it has been observed that thermal resistance is better due to the decrease in mass loss in the thermal degradation step. It was observed that the composite containing FF with alkali modification improved the thermal resistance of pure PBS the best.

### 3.6 | Thermo-Mechanical Properties of Composites

The storage modulus curves of PBS and PBS/FF composites are shown in Figure 7a, and  $\tan \delta$  curves of PBS and PBS/FF composites are shown in Figure 7b. The storage modulus values of PBS composites containing FF were significantly

higher than the storage modulus of PBS both before and after the glass transition temperature ( $T_g$ ). This increase is approximately twice as high as the storage modulus of PBS in the composites. This increase in the storage modulus is thought to be due to the restriction of the movement of the polymer chains by fiber loading [64–67]. In order to have stronger interfacial adhesion between the matrix and the filler, the height of the  $\tan \delta$  peaks should be low [68, 69]. According to the  $\tan \delta$  curves of PBS/FF composites, no widening of the  $\tan \delta$  band was observed, similar to PBS without additives. It is observed that the height of the  $\tan \delta$  peak at its maximum point decreases with the addition of unmodified and modified FF. Composites containing FF showed lower  $\tan \delta$  values compared to PBS and additionally showed a decrease in peak  $\tan \delta$  temperature. The reason for the strong interface adhesion between PBS and ES-FF in SEM micrographs is that the PBS/ES-FF sample gave the lowest peak  $\tan \delta$  value among the composites with a slight difference. It was observed that the SEM images and  $\tan \delta$  results supported each other.

### 3.7 | Biodegradability of Composites

Due to the high resistance to degradation (environmental conditions or biological agents) of the thermoplastic polymers, the

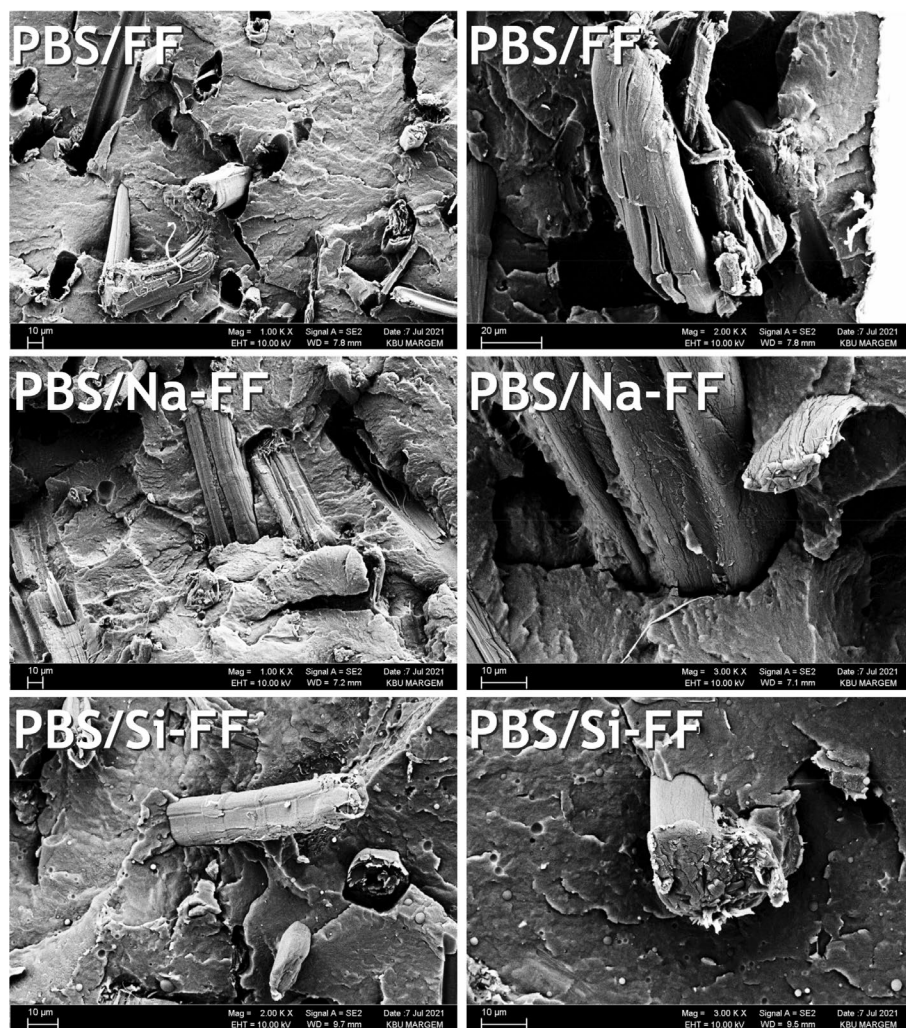


**FIGURE 10** | SEM micro-images of composites.



studied samples were exposed under controlled conditions to a biodegradation test with *Chaetomium globosum* for the period of 9 weeks.

After the degradation period, the composite samples (PBS/Na-FF, PBS/FF, and PBS/Si-FF) were very soft, breaking very easily (with bare hands), while the mass loss reached a percent of up to about 18% from the initial mass, a value recorded for the PBS/Na-FF sample (Figure 8). As expected, the lower degradation rate was recorded for the pure PBS sample of about 4% mass loss from the initial mass. Figure 9 represents the infrared spectra in the fingerprint region ( $1830\text{--}500\text{ cm}^{-1}$ ) of the composite materials.

The spectra of the polymer composites are very similar to the PBS spectrum, as the bands from the fibers overlap with the bands from the polymer. After biodegradation, the differences appearing in the biodegraded samples compared to non-biodegraded ones are mainly due to defects in the surface morphology as well as remaining fungal hyphae. The spectra of biodegraded samples, compared to non-biodegraded ones, show main differences for the bands from  $1616$ ,  $1335$ ,  $1313$ , and  $1156\text{ cm}^{-1}$  (assigned to which stretching vibrations of the water molecules, and to CH and C—O stretching vibrations) increase in intensity, while the bands from  $1269$ ,  $1245$ , and  $1207\text{ cm}^{-1}$  (assigned to C=O and C—O stretching vibrations) present a slight decrease in intensity with the increase of the exposure period to degradation factors. The increased intensity of the bands assigned to CH and C—O stretching vibrations is most probably due to the presence of the organic matter from the remaining fungal hyphae at the surface of the composites, but also to the formation of free C—O radicals due to the break of the internal bonds. These soften the composites and also make them more hydrophilic.

### 3.8 | Morphological Evidence of Composites

When the FESEM images of the composite structures shown in Figure 10 are analyzed, it is clearly seen that the unmodified FF-containing composite has gaps between the fiber and the matrix, indicating weak adhesion. The FESEM images of the composites containing Na-FF and ES-FF showed that the adhesion between the matrix and the surface-modified FF was relatively stronger and covered the surface. This observation indicates that alkalization and silanization treatments significantly improve the interfacial adhesion between flax fiber and polymer matrix [70–72]. The best interfacial interaction was observed in the sample with surface modification by silanization.

## 4 | Conclusion

Composite materials were obtained by adding flax fiber with alkalization and silanization surface modifications to pure PBS, which is environmentally friendly, biodegradable, and unmodified, at the determined ratios. As the peaks in the FTIR graphs of the FF fibers are examined, it is seen that the silanization and alkalization surface modification processes are successfully performed. FESEM images of FF samples visually revealed that the surface roughness increased after the surface modification processes and the FF fiber walls were coated with silane groups.

Based on the morphological studies of PBS/FF composites by SEM images, it was found that alkalization and silanization processes between PBS and FF greatly improved the interfacial adhesion. The best interfacial interaction was observed in the sample with surface modification by silanization. As a result of the water absorption test applied to the composite and PBS samples, the silanization-modified FF-containing composite structures showed the highest water absorption capacity. According to the tensile test data, there was no significant difference in tensile strength with the addition of FF to pure PBS, while a decrease in elongation at break and an increase in Young's modulus were observed compared to pure PBS. The specific wear resistance of the composite modified by silanization showed the best performance. The storage modulus plots obtained by DMA test revealed that the storage modulus values of PBS composites containing FF were higher than the storage modulus of pure PBS.  $\tan \delta$  curves claimed that FF-containing composites showed lower  $\tan \delta$  values than PBS and decreased peak  $\tan \delta$  temperature. When the TGA diagrams of FF fibers were examined, the degradation rate after the silanization surface modification process was found to be low compared to other samples. According to the TGA graphs of PBS/FF composites, silane-treated FF loading slightly increased the thermal strength of the composite. Compared to PBS without additives, the composites exhibited lower thermal strength. Since the outdoor applications of polymeric films contain limitations related to physical properties, enhancement in interface adhesion of FF to PBS expanded its use in related fields by increasing mechanical and physical durability. Different surface modification routes can be applied to enhance PBS-FF compatibility in future works.

### Author Contributions

**Sema Özalp:** investigation, methodology, formal analysis, writing – original draft, writing – review and editing, validation. **Sedef Sismanoglu:** writing – review and editing, writing – original draft, investigation, formal analysis. **Ümit Tayfun:** writing – original draft, writing – review and editing, investigation, supervision, methodology, formal analysis. **Carmen-Mihaela Popescu:** writing – original draft, writing – review and editing, investigation, formal analysis. **Fazilat B. Kairliyeva:** writing – original draft, formal analysis. **Yasin Kanbur:** writing – original draft, writing – review and editing, investigation, supervision, project administration, methodology, conceptualization, formal analysis, funding acquisition.

### Conflicts of Interest

The authors declare no conflicts of interest.

### Data Availability Statement

The data that support the findings of this study are available on request from the corresponding author. The data are not publicly available due to privacy or ethical restrictions.

### References

1. R. Sobhan, A. Mustari, P. Chakma, and N. R. Dhar, “An Overview: Natural Fiber Composites as Eco-Friendly Materials, Their Properties, Chemical Treatments, Applications,” *Recent Advancements in Mechanical Engineering: Select Proceedings of ICRAME 2021* (2023): 459–471.
2. A. Ramachandran, S. Mavinkere Rangappa, V. Kushvaha, A. Khan, S. Seingchin, and H. N. Dhakal, “Modification of Fibers and Matrices

- in Natural Fiber Reinforced Polymer Composites: A Comprehensive Review," *Macromolecular Rapid Communications* 43 (2022): 2100862.
3. M. Wróbel-Kwiatkowska, M. Kropiwnicki, and W. Rymowicz, *Handbook of Composites From Renewable Materials* (Wiley, 2017), 283–301.
4. Ş. Yıldızhan, A. Çalık, M. Özcanlı, and H. Serin, "Bio-Composite Materials: A Short Review of Recent Trends, Mechanical and Chemical Properties, and Applications," *European Mechanical Science* 2 (2018): 83–91.
5. Y. El Moussi, B. Otazaghine, A.-S. Caro-Bretelle, R. Sonnier, A. Taguet, and N. Le Moigne, "Controlling Interfacial Interactions in LDPE/Flax Fibre Biocomposites by a Combined Chemical and Radiation-Induced Grafting Approach," *Cellulose* 27 (2020): 6333–6351.
6. M. Ramesh, L. Rajeshkumar, D. Balaji, and V. Bhuvaneshwari, "Keratin-Based Biofibers and Their Composites," In *Advances in Bio-Based Fiber*, vol. 52 (Woodhead Publishing, 2022), 315–334.
7. A. P. More, "Flax Fiber-Based Polymer Composites: A Review," *Advanced Composites and Hybrid Materials* 5 (2022): 1–20.
8. M. R. M. Asyraf, M. R. Ishak, M. N. F. Norrahim, et al., "Potential of Flax Fiber Reinforced Biopolymer Composites for Cross-Arm Application in Transmission Tower: A Review," *Fibers and Polymers* 23 (2022): 853–877.
9. M. Akonda, S. Alimuzzaman, D. U. Shah, and A. N. M. Rahman, "Physico-Mechanical, Thermal and Biodegradation Performance of Random Flax/Poly(lactic Acid) and Unidirectional Flax/Poly(lactic Acid) Biocomposites," *Fibers* 6 (2018): 98.
10. L. Aliotta, V. Gigante, M.-B. Coltelli, P. Cinelli, A. Lazzeri, and M. Seggiani, "Thermo-Mechanical Properties of PLA/Short Flax Fiber Biocomposites," *Applied Sciences* 9 (2019): 3797.
11. W. Gieparda, S. Rojewski, and W. Róžańska, "Effectiveness of Silanization and Plasma Treatment in the Improvement of Selected Flax Fibers' Properties," *Materials* 14 (2021): 3564.
12. M. Kodal, Z. D. Topuk, and G. Ozkoc, "Dual Effect of Chemical Modification and Polymer Precoating of Flax Fibers on the Properties of Short Flax Fiber/Poly(Lactic Acid) Composites," *Journal of Applied Polymer Science* 132 (2015).
13. F. Rothenhäusler, A. Ouali, R. Rinberg, M. Demleitner, L. Kroll, and H. Ruckdaeschel, "Influence of Sodium Hydroxide, Silane, and Siloxane Treatments on the Moisture Sensitivity and Mechanical Properties of Flax Fiber Composites," *Polymer Composites* 45 (2024): 8937–8948.
14. P. Pei, R. Zou, X. Wang, et al., "Biocomposite Optimization With NaOH-Modified Bagasse Fiber, Polybutylene Succinate, and Poly(Lactic Acid) Using RSM Approach," *BioResources* 18 (2023): 5683–5702.
15. W. Frącz, G. Janowski, and Ł. Bąk, "Influence of the Alkali Treatment of Flax and Hemp Fibers on the Properties of PHBV Based Biocomposites," *Polymers* 13 (2021): 1965.
16. S. Alimuzzaman, R. H. Gong, and M. Akonda, "Biodegradability of Nonwoven Flax Fiber Reinforced Poly(lactic Acid) Biocomposites," *Polymer Composites* 35 (2014): 2094–2102.
17. A. Iwańczuk, M. Kozłowski, M. Łukaszewicz, and S. Jabłoński, "Anaerobic Biodegradation of Polymer Composites Filled With Natural Fibers," *Journal of Polymers and the Environment* 23 (2015): 277–282.
18. I. I. Shuvo and M. Shadhin, "Biopolymer Flax (*Linum usitatissimum* L.) and Its Prospects in Biodegradable Composite Fabrication—A Short Review," *Journal of Textile Engineering & Fashion Technology* 5 (2019): 267–274.
19. K. Charlet, J.-P. Jernot, M. Gomina, L. Bizet, and J. Bréard, "Mechanical Properties of Flax Fibers and of the Derived Unidirectional Composites," *Journal of Composite Materials* 44 (2010): 2887–2896.
20. M. J. Mochane, S. I. Magagula, J. S. Sefadi, and T. C. Mokhena, "A Review on Green Composites Based on Natural Fiber-Reinforced Polybutylene Succinate (PBS)," *Polymers (Basel)* 13 (2021): 1200.
21. M. Puchalski, G. Szparaga, T. Biela, A. Gutowska, S. Sztajnowski, and I. Krucińska, "Molecular and Supramolecular Changes in Polybutylene Succinate (PBS) and Polybutylene Succinate Adipate (PBSA) Copolymer During Degradation in Various Environmental Conditions," *Polymers (Basel)* 10 (2018): 251.
22. S. Islam, M. B. Hasan, F. E. Karim, et al., "Thermoset and Thermoplastic Polymer Composites Reinforced With Flax Fiber: Properties and Application—A Review," *SPE Polymers* 6 (2025): e10172.
23. M. Rahimi, A. Omran, and A. Tagnit-Hamou, "Role of Homogenization and Surface Treatment of Flax Fiber on Performance of Cement-Based Composites," *Cleaner Materials* 3 (2022): 100037.
24. I. Van de Weyenberg, T. Chi Truong, B. Vangrimde, and I. Verpoest, "Improving the Properties of UD Flax Fibre Reinforced Composites by Applying an Alkaline Fibre Treatment," *Composites. Part A, Applied Science and Manufacturing* 37 (2006): 1368–1376.
25. P. Georgiopoulos, A. Christopoulos, S. Koutsoumpis, and E. Kontou, "The Effect of Surface Treatment on the Performance of Flax/Biodegradable Composites," *Composites Part B: Engineering* 106 (2016): 88–98.
26. J. Biagiotti, D. Puglia, L. Torre, et al., "A Systematic Investigation on the Influence of the Chemical Treatment of Natural Fibers on the Properties of Their Polymer Matrix Composites," *Polymer Composites* 25 (2004): 470–479.
27. S. W. Azhar, F. Xu, Y. Zhang, and Y. Qiu, "Fabrication and Mechanical Properties of Flaxseed Fiber Bundle-Reinforced Polybutylene Succinate Composites," *Journal of Industrial Textiles* 50 (2020): 98–113.
28. M. Sarikanat, Y. Seki, K. Sever, E. Bozaci, A. Demir, and E. Ozdogan, "The Effect of Argon and Air Plasma Treatment of Flax Fiber on Mechanical Properties of Reinforced Polyester Composite," *Journal of Industrial Textiles* 45 (2016): 1252–1267.
29. H. A. Raslan, M. Y. Elnaggar, and E. S. Fathy, "Effect of Gamma Irradiation on the Waste Polyethylene/Bagasse Composites Reinforced With Flax and Sisal Fibers for Use in Wood Applications," *Journal of Vinyl and Additive Technology* 30 (2024): 201–216.
30. X. Wang, Y. Cui, Q. Xu, B. Xie, and W. Li, "Effects of Alkali and Silane Treatment on the Mechanical Properties of Jute-Fiber-Reinforced Recycled Polypropylene Composites," *Journal of Vinyl and Additive Technology* 16 (2010): 183–188.
31. A. J. Basbasan, B. Hararak, C. Winotapun, et al., "Lignin Nanoparticles for Enhancing Physicochemical and Antimicrobial Properties of Polybutylene Succinate/Thymol Composite Film for Active Packaging," *Polymers* 15 (2023): 989.
32. G. Dorez, A. Taguet, L. Ferry, and J. M. Lopez-Cuesta, "Thermal and Fire Behavior of Natural Fibers/PBS Biocomposites," *Polymer Degradation and Stability* 98 (2013): 87–95.
33. J.-M. Wang, H. Wang, E.-C. Chen, Y.-J. Chen, and T.-M. Wu, "Role of Organically-Modified Zn-Ti Layered Double Hydroxides in Poly(Butylene Succinate-Co-Adipate) Composites: Enhanced Material Properties and Photodegradation Protection," *Polymers (Basel)* 13 (2021): 2181.
34. C.-F. J. Kuo, W. L. Lan, S. H. Chen, and C.-Y. Chen, "Property Modification and Process Parameter Optimization Design of Poly(lactic Acid) Composite Materials Part II: Application of Response Surface Methodology and Multi-Objective Particle Swarm Optimization in the Processing of Poly(lactic Acid) Composite Fiber," *Textile Research Journal* 85 (2015): 687–700.
35. G. F. Moore and S. M. Saunders, *Advances in Biodegradable Polymers*, vol. 9 (Rapra Technology Ltd, 1998).
36. S. A. Rafiqah, A. Khalina, A. S. Harmaen, et al., "A Review on Properties and Application of Bio-Based Poly(Butylene Succinate)," *Polymers (Basel)* 13 (2021): 1436.
37. E. Frollini, N. Bartolucci, L. Sisti, and A. Celli, "Poly(Butylene Succinate) Reinforced With Different Lignocellulosic Fibers," *Industrial Crops and Products* 45 (2013): 160–169.

38. O. Platnieks, S. Gaidukovs, V. Kumar Thakur, A. Barkane, and S. Beluns, "Bio-Based Poly (Butylene Succinate): Recent Progress, Challenges and Future Opportunities," *European Polymer Journal* 161 (2021): 110855.
39. A. Bourmaud, Y. M. Corre, and C. Baley, "Fully Biodegradable Composites: Use of Poly-(Butylene-Succinate) as a Matrix and to Plasticize l-Poly-(Lactide)-Flax Blends," *Industrial Crops and Products* 64 (2015): 251–257.
40. N. Ketata, B. Seantier, N. Guermazi, and Y. Grohens, "On the Development of a Green Composites Based on Poly (Lactic Acid)/Poly (Butylene Succinate) Blend Matrix Reinforced by Long Flax Fibers," *Materials Today Proceedings* 52 (2021): 95–103.
41. J. Pawar, R. Malagi, and M. Jadhav, "Modeling of Copperremoval From Simulated Wastewater by Adsorption on to Fungal Biomass Using Artificial Neural network," *Journal of the Chinese Institute of Engineers, Transactions of the Chinese Institute of Engineers, Series A* 5 (2025): 35–44.
42. E. Cebe and A. B. İrez, "Development of Hybrid Polymer Composites With Improved Thermal Properties and Investigation of Their Mechanical Properties for Battery Module Case Manufacturing in Electric Vehicles," *International Journal of Advances in Engineering and Pure Sciences* 36, no. 3 (2024): 224–234.
43. Ö. Şengül, M. Şeremet, and M. Kam, "Sürdürülebilir Üretim İçin Grafit Takviyeli Polipropilen Kompozit Ürünlerin Bazı Termal ve Mekanik Özelliklerinin Deneysel Analizi," *Bilecik Şeyh Edebali Üniversitesi Fen Bilimleri Dergisi* 7 (2020): 10–20.
44. E. Robles, N. Izaguirre, B.-I. Dogaru, C.-M. Popescu, I. Barandiaran, and J. Labidi, "Sonochemical Production of Nanoscaled Crystalline Cellulose Using Organic Acids," *Green Chemistry* 22 (2020): 4627–4639.
45. C. Popescu, D. Jones, D. Kržišnik, and M. Humar, "Determination of the Effectiveness of a Combined Thermal/Chemical Wood Modification by the Use of FT-IR Spectroscopy and Chemometric Methods," *Journal of Molecular Structure* 1200 (2020): 127133.
46. M. Broda, I. Dąbek, A. Dutkiewicz, et al., "Organosilicons of Different Molecular Size and Chemical Structure as Consolidants for Waterlogged Archaeological Wood – A New Reversible and Retreatable Method," *Scientific Reports* 10, no. 1 (2020): 2188.
47. C. M. Popescu and M. Broda, "Interactions Between Different Organosilicons and Archaeological Waterlogged Wood Evaluated by Infrared Spectroscopy," *Forests* 12 (2021): 268.
48. N. S. Nor Arman, R. S. Chen, and S. Ahmad, "Review of State-of-the-Art Studies on the Water Absorption Capacity of Agricultural Fiber-Reinforced Polymer Composites for Sustainable Construction," *Construction and Building Materials* 302 (2021): 124174.
49. O. Yildirimkaraman, U. H. Yildiz, A. O. Akar, and U. Tayfun, "Evaluation of Water Repellency in Bentonite Filled Polypropylene Composites via Physical and Mechanical Methods," *IOP SciNotes* 1 (2020): 024804.
50. S. Shahinur, M. Hasan, Q. Ahsan, N. Sultana, Z. Ahmed, and J. Haider, "Effect of Rot-, Fire-, and Water-Retardant Treatments on Jute Fiber and Their Associated Thermoplastic Composites: A Study by FTIR," *Polymers (Basel)* 13 (2021): 2571.
51. S. N. Kartal, S. Aysal, E. Terzi, N. Yilgör, T. Yoshimura, and K. Tsunoda, "Wood and Bamboo-PP Composites: Fungal and Termite Resistance, Water Absorption, and FT-IR Analyses," *BioResources* 8 (2013): 1222–1244.
52. Y. Ji, X. Liu, X. Liu, et al., "An Environmentally Friendly and Highly Efficient PBS Composite Membrane Prepared by TiO<sub>2</sub> Hybridization and PDA Surface Coating," *Journal of Environmental Chemical Engineering* 13 (2025): 115033.
53. H. Ku, H. Wang, N. Pattarachaiyakooop, and M. Trada, "A Review on the Tensile Properties of Natural Fiber Reinforced Polymer Composites," *Composites Part B: Engineering* 42 (2011): 856–873.
54. J. Vercher, V. Fombuena, A. Diaz, and M. Soriano, "Influence of Fibre and Matrix Characteristics on Properties and Durability of Wood-Plastic Composites in Outdoor Applications," *Journal of Thermoplastic Composite Materials* 33 (2020): 477–500.
55. S. Sismanoglu, Ü. Tayfun, P. Gradinariu, C. M. Popescu, and Y. Kanbur, "Reuse of Black Cumin Biomass Into Beneficial Additive for Thermoplastic Polyurethane-Based Green Composites With Silane Modifiers," *Biomass Conversion and Biorefinery* 13 (2023): 14169–14184.
56. S. Polat, Y. Sun, E. Çevik, H. Colijn, and M. E. Turan, "Investigation of Wear and Corrosion Behavior of Graphene Nanoplatelet-Coated B4C Reinforced Al–Si Matrix Semi-Ceramic Hybrid Composites," *Journal of Composite Materials* 53 (2019): 3549–3565.
57. S. T. Mohamed, S. Tirkes, A. O. Akar, and U. Tayfun, "Hybrid Nanocomposites of Elastomeric Polyurethane Containing Halloysite Nanotubes and POSS Nanoparticles: Tensile, Hardness, Damping and Abrasion Performance," *Clay Minerals* 55 (2020): 281–292.
58. Y. Zhong, U. Kureemun, L. Q. N. Tran, and H. P. Lee, "Natural Plant Fiber Composites-Constituent Properties and Challenges in Numerical Modeling and Simulations," *International Journal of Applied Mechanics* 09 (2017): 1750045.
59. S. Radoor, J. Karayil, S. M. Rangappa, S. Siengchin, and J. Parameswaranpillai, "A Review on the Extraction of Pineapple, Sisal and Abaca Fibers and Their Use as Reinforcement in Polymer Matrix," *Express Polymer Letters* 14 (2020): 309–335.
60. M. Sorieul, A. Dickson, S. Hill, and H. Pearson, "Plant Fibre: Molecular Structure and Biomechanical Properties, of a Complex Living Material, Influencing Its Deconstruction Towards a Biobased Composite," *Materials* 9 (2016): 618.
61. Z. Qiu, M. Komura, T. Ikehara, and T. Nishi, "DSC and TMDSC Study of Melting Behaviour of Poly(Butylene Succinate) and Poly(Ethylene Succinate)," *Polymer* 44 (2003): 7781–7785.
62. K. Chrissafis, K. M. Paraskevopoulos, and D. N. Bikiaris, "Thermal Degradation Mechanism of Poly(Ethylene Succinate) and Poly(Butylene Succinate): Comparative Study," *Thermochimica Acta* 435 (2005): 142–150.
63. R. Chen, W. Zou, H. Zhang, G. Zhang, and J. Qu, "Crystallization Behavior and Thermal Stability of Poly(Butylene Succinate)/Poly(Propylene Carbonate) Blends Prepared by Novel Vane Extruder," *AIP Conference Proceedings* 1713 (2016): 050002.
64. X. Wang and M. Petrú, "Effect of Hygrothermal Aging and Surface Treatment on the Dynamic Mechanical Behavior of Flax Fiber Reinforced Composites," *Materials* 12 (2019): 2376.
65. U. Tayfun, M. Dogan, and E. Bayramli, "Influence of Surface Modifications of Flax Fiber on Mechanical and Flow Properties of Thermoplastic Polyurethane Based Eco-Composites," *Journal of Natural Fibers* 13 (2016): 309–320.
66. M. Aravindh, S. Sathish, L. Prabhu, et al., "Effect of Various Factors on Plant Fibre-Reinforced Composites With Nanofillers and Its Industrial Applications: A Critical Review," *Journal of Nanomaterials* 2022 (2022): 4455106.
67. M. T. Hayajneh, M. M. Al-Shrida, and F. M. AL-Oqla, "Mechanical, Thermal, and Tribological Characterization of Bio-Polymeric Composites: A Comprehensive Review," *E-Polymers* 22 (2022): 641–663.
68. S. Yang, J. Taha-Tijerina, V. Serrato-Diaz, K. Hernandez, and K. Lozano, "Dynamic Mechanical and Thermal Analysis of Aligned Vapor Grown Carbon Nanofiber Reinforced Polyethylene," *Composites Part B: Engineering* 38 (2007): 228–235.
69. C. Arslan and M. Dogan, "The Effects of Fiber Silane Modification on the Mechanical Performance of Chopped Basalt Fiber/ABS Composites," *Journal of Thermoplastic Composite Materials* 33 (2019): 1449–1465.



70. Ü. Tayfun, "Application of Sustainable Treatments to Fiber Surface for Performance Improvement of Elastomeric Polyurethane Reinforced With Basalt Fiber," *Journal of Vinyl and Additive Technology* 29 (2023): 1036–1045.
71. M. S. Ullah, R. Yildirim, M. Kodai, and G. Ozkoc, "Reactive Compatibilization of PLA/PBSbio-Blends via a New Generation of Hybrid Nanoparticles," *Journal of Vinyl and Additive Technology* 29 (2023): 737–757.
72. N. Sato, T. Kurauchi, S. Sato, and O. Kamigaito, "Microfailure Behaviour of Randomly Dispersed Short Fibre Reinforced Thermoplastic Composites Obtained by Direct SEM Observation," *Journal of Materials Science* 26 (1991): 3891–3898.